Energy Conversion and Management 88 (2014) 723–731

Contents lists available at ScienceDirect

Energy Conversion and Management

journal homepage: www.elsevier.com/locate/enconman

Thermodynamic analysis of an HCCI engine based system running on natural gas

Mohamed Djermouni, Ahmed Ouadha *

Laboratoire d'Energie et Propulsion Navale, Faculté de Génie Mécanique, Université des Sciences et de la Technologie Mohamed BOUDIAF d'Oran, B.P. 1505 Oran El-M'naouar, 31000 Oran, Algeria

ARTICLE INFO

Article history:
Received 28 March 2014
Accepted 10 September 2014

Keywords:
HCCI engine
Natural gas
Thermodynamic analysis

ABSTRACT

This paper attempts to carry out a thermodynamic analysis of a system composed of a turbocharged HCCI engine, a mixer, a regenerator and a catalytic converter within the meaning of the first and the second law of thermodynamics. For this purpose, a thermodynamic model has been developed taking into account the gas composition resulting from the combustion process and the specific heat temperature dependency of the working fluid. The analysis aims in particular to examine the influence of the compressor pressure ratio, ambient temperature, equivalence ratio, engine speed and the compressor isentropic efficiency on the performance of the HCCI engine. Results show that thermal and exergetic efficiencies increase with increasing the compressor pressure ratio. However, the increase of the ambient temperature involves a decrease of the engine efficiencies. Furthermore, the variation of the equivalence ratio improves considerably both thermal and exergetic efficiencies. As expected, the increase of the engine speed enhances the engine performances. Finally, an exergy losses mapping of the system show that the maximum exergy losses occurs in the HCCI engine.

1. Introduction

Compared to gasoline engines, Diesel engines have many advantages, such as simplicity, high performance, ease maintenance, low fuel costs, low consumption, high compression ratio, high power/weight ratio and durability. However, emissions from these engines are considered one of the main sources of air pollution that seriously threaten our environment. Efforts to reduce these emissions, especially particulate matter and nitrogen oxides, are necessary for the preservation of the environment, human health, welfare and prosperity.

Consequently, the dual requirements of better thermal efficiency and increasingly rigorous emissions restrictions have been driven, in recent years, Diesel engines manufacturers to forward a number of technological solutions, such as water addition, internal engine modification, aftertreatment and alternative fuels [1]. Another promising solution has been focused on combustion mode that benefits from advantages of conventional Diesel and spark ignition engines in order to reduce pollutant emissions. This objective can be achieved using homogeneous charge compression ignition (HCCI) technology.

HCCI engines combine characteristics of both spark-ignited engines and diesel engines. Similar to sparkignited engines, HCCI uses a pre-mixed fuel-in-air charge, and similar to diesel engines, the mixture is compression ignited. The diluted premixed charge facilitates a relatively uniform auto-ignition event rather than a non-premixed flame found in diesel engines, and thus HCCI engines can achieve fewer emissions of particulate matter. Homogeneous charge compression ignition, when applied to a gasoline engine, offers the potential for a noticeable improvement in fuel economy and dramatic reductions in NOx emissions as compared to the spark ignition operation. Indeed, it has been demonstrated that it can achieve fuel economy levels comparable to those of a diesel engine with low NOx emissions [2]. HCCI engines run on lean air–fuel mixtures which are auto-ignited by compression. Using lean air–fuel mixtures, the combustion produces less nitric oxides (NOx) and particulate matter (PM) emissions, while simultaneously achieving high thermal efficiency as compared to conventional Diesel and spark ignition [3]. Further, HCCI combustion is mainly governed by chemical kinetics. It excludes the rescues to external means of direct ignition control which make it difficult to control engine operation over a wide load-speed range. Adjusting inlet temperature or pressure of the mixture and variation of compression ratio can help to control ignition and combustion intensity [4].

* Corresponding author. Tel.: +213 661 204 325; fax: +213 41 290 466.
E-mail address: ah_ouadha@yahoo.fr (A. Ouadha).

http://dx.doi.org/10.1016/j.enconman.2014.09.033
0196-8904/

Nomenclature

c_p	specific heat at constant pressure (kJ/kg)
$\dot{E}x$	exergy rate (kW)
ex	specific exergy (kJ/kg)
f	residual gas fraction
H	enthalpy (kJ)
h	specific enthalpy (kJ/kg)
$\dot{m}$	mass flow rate (kg/s)
N	engine speed (rpm)
p	pressure (bar)
r_c	engine compression ratio
r_p	compressor pressure ratio
$\dot{Q}$	rate of heat (kW)
R	molar gas constant (J/mol K)
s	specific entropy (kJ/kg)
T	temperature (K)
$\dot{W}$	power rate (kW)
w	specific work (kJ/kg)

Greek symbols

$\Delta\dot{E}x$	exergy losses rate (kW)
ε	effectiveness
η	efficiency

Subscripts

a	air
ch	chemical
$comb$	combustion
$comp$	compressor/compression
ex	exergetic
f	fuel
in	supplied
l	losses
out	rejected
ph	physical
t	total
th	thermal
0	environment state

As Diesel costs increase, ship owners are seeking alternative and cleaner fuels to move their ships. Among the most promising source of energy, natural gas is probably the most serious option at present and the near future for marine applications as the other fuels such as biofuels and hydrogen are too expensive at present. Natural gas is an abundant source of energy which is currently priced significantly lower than distillate and residual petroleum fuels. It has the potential to provide similar performance to diesel with low emissions. Natural gas has a wide flammability range (5.3–15) against 0.6–5.5 for Diesel fuel and 1–7.6 for gasoline fuel allowing a lean mixture in the engines. It burns slowly with a low flame temperature of 1790 °C against 1977 °C for gasoline [5]. The natural gas combustion in the diesel engines produces very low levels of CO and particulate emissions. It does not have an effect on the level of HC emissions [6]. Further, natural gas requires minimum mixture preparation, and is chemically stable, both of which make it suitable for the HCCI concept. However, natural gas is hard to auto-ignite and therefore requires a higher compression ratio, some amount of intake heating, or some type of pre-ignition [7].

In order to use efficiently and effectively the energy resources, recent analyses join quality to quantity of the energy used to realise a given purpose. In other words, associate the second law of thermodynamics which deals with the quality to the first law of thermodynamics dealing with the quantity of energy. The exergy, defined as the amount of energy which can be extracted as useful work, can be used to assess the quality of energy resource. A thermodynamic analysis based on both the first and the second laws of thermodynamics can be used in order to evaluate the theoretical performance of the system. Using this thermodynamic modelling, it is easy to predict the thermal efficiency, the exergy losses and the exergy efficiency of the system. Although that this analysis is theoretic, it can reduce considerably the number of experimental tests to be realised, which are usually costly and time consuming.

Several experimental, numerical and analytical studies have been devoted to investigate and understand HCCI engines [8–22]. However, the literature seems to contain few investigations on thermodynamic analysis of these engines. Among the few studies published recently, Soylu [23] has used a zero dimensional thermodynamic model that contains a simple heat release sub-model and an autoignition model in a predictive fashion to better understand the in-cylinder processes and the efficiency potential of a natural gas engine in the HCCI mode. The model has been also used for parametric studies to evaluate HCCI control strategies that can be tested on the research engine. The results indicated that if the initial conditions of the mixture are known precisely at intake valve closing, the autoignition timing is controllable. Khaliq et al. [24] have applied a combined first and second law of thermodynamic approach for a HCCI engine operating on wet ethanol. They investigated the effects of turbocharger compressor ratio, ambient temperature, and compressor adiabatic efficiency on first law efficiency, second law efficiency, and exergy destruction in each component. They showed that the effect of turbocharger pressure ratio on exergy destruction is more significant than compressor efficiency and ambient temperature. In addition, most of exergy losses (90.09%) occur in HCCI engine. Khaliq and Trivedi [25] have presented first and second law analyses of a new combined power cycle based on wet ethanol fuelled HCCI engine and an organic Rankine cycle. The authors found that first law efficiency and second law efficiency of the combined power cycle significantly vary with the change in the turbocharger pressure ratio, but the change in pinch point temperature, turbocharger efficiency, and ambient temperature shows small variations in these efficiencies. They showed also that the biggest exergy loss occurs in the HCCI engine (68.7%). In order to understand how the exergy losses change with different HCCI engine operating conditions, Saxena et al. [26] have coupled a crank-angle resolved exergy analysis methodology with a multi-zone chemical kinetic model of a gasoline-fuelled HCCI engine.

Although there are several studies on HCCI engines as cited above, thermodynamic analyses of these devices are scarce. Therefore, thermodynamic modelling and analysis of HCCI engines based systems are highly needed for calculating their overall performance. This analysis is useful for optimal design purposes. It can, in some cases, minimise and direct tests on real models by guiding experimental research and engine development.

The purpose of this study is to conduct a thermodynamic analysis of a HCCI engine using simultaneously the first and second law of thermodynamics. The latter, through the concept of exergy, quantifies exergy losses and their location in the system.

2. Working fluid thermodynamic properties

Thermodynamic cycle calculations, an important phase in the design and development of internal combustion engines, require the knowledge of combustion products composition and their thermodynamic properties. These properties are necessary to investigate both design-point and off-design performances, and to determine optimum design parameters. Generally, the in-cylinder working fluid is considered as simply air. However, more rigorous thermodynamic studies require taking into account changes in the gas composition by tracking several chemical species.

In real processes, the specific heat of gases varies with temperature. However, for engine applications, its variation is negligible with pressure. The latter is moderate. In the present model, it is assumed that the specific heat of gases varies with temperature according to the following polynomials form:

$$c_p = \sum_{i=1}^{11} a_i T^i \tag{1}$$

The numerical coefficients a_i, for each species, have been determined by a regression analysis method using literature data for temperature ranging from 300 to 3000 K [27].

Enthalpy and entropy can be derived from the specific heat capacity using the following relations:

$$\begin{cases} h = h_{00} + \int c_p(T)dT \\ s = s_{00} + \int \frac{c_p(T)}{T} dT - r\ln(p) \end{cases} \tag{2}$$

where h_{00} and s_{00} are the integration constants calculated according to an arbitrary reference state. For each gas, the enthalpy constant of integration is the sum of two parts: a part calculated by adjusting $h = 0$ at 298 K and a part representing the enthalpy of formation of the gas. For entropy, the integration constant is calculated by adjusting $s = 0$ at 298 K and 1.01325 bar.

Thermodynamic properties of the combustion products have different dependencies on temperature. Therefore, it is more appropriate to calculate the thermodynamic properties of their mixture as a sum of the properties of individual species:

$$\Phi_m = \sum_{i=1}^{n} \Phi_i x_i \tag{3}$$

Under ideal conditions, the combustion of fuels produces only water (H_2O) and carbon dioxide (CO_2), in addition to the nitrogen (N_2) from the air. However, in a real combustion, in addition to these main combustion products, the engine exhaust gases also contain many others compounds. In the present work, the following species are considered as combustion products: CO_2, CO, H_2O, N_2, O_2 and H_2. The equation for combustion of natural gas is simplified by considering a single reaction of methane, the main component of natural gas, with air:

$$\mathrm{CH_4} + \left(\frac{2}{\phi}\right)(\mathrm{O_2} + 3.76\mathrm{N_2}) \rightarrow n_1\mathrm{CO_2} + n_2\mathrm{H_2O} + n_3\mathrm{N_2} + n_4\mathrm{O_2} + n_5\mathrm{CO} + n_6\mathrm{H_2} \tag{4}$$

The mole fractions, n_i, of the combustion products have been determined under equilibrium conditions by solving a nonlinear system of seven equations (six molar fractions and the total number of moles of products). The equilibrium constants are calculated as function of the temperature at the end of the combustion process.

3. Thermodynamic analysis

Habitually, thermal systems are analysed using the energy analysis method which is based on the first law of thermodynamics, i.e. the energy conservation concept. Unfortunately, this method cannot locate the degradation of the quality of energy. Instead, exergy analysis which is based on both the first and second laws of thermodynamics can overcome easily the limitations of the energy analysis. It permits to quantify the magnitude and the location of exergy losses within the system. Furthermore, the total exergy losses can be considered as an optimisation criteria which, by minimisation, provides optimum processes configuration. The concept and the methodology of exergy analysis are well-documented in the literature.

For both energy and exergy analysis, the thermodynamic model is based on the following assumptions:

- All processes are marked by steady state and steady flow,
- Kinetic and potential energy have negligible effects,
- The temperature and pressure of the environment are 25 °C and 1 atm, respectively.

3.1. System description

The system considered in the present study is depicted in Fig. 1. Methane is used as the fuel, since it is the main constituent of natural gas. The system consists of a compressor, a regenerator, a mixer, an HCCI engine, a catalytic converter and a turbine. Ambient air enters the compressor where its pressure and temperature rise to reach p_2 and T_2. The compressed air passes through a generator where it is heated to T_3 at constant pressure. The inlet air must be heated significantly to ensure fuel autoignition. The variation of inlet air temperature can be achieved by controlling the amount of exhaust gases that enter the regenerator using controllable valve. The hot air exiting the regenerator is mixed with natural gas injected into a mixer to form homogeneous mixture. Thus, the homogeneous gas mixture formed enters the combustion chamber where conditions of temperature and pressure reached during the compression process ensure an auto-ignition of the charge by approaching the top dead centre. Then, the exhaust gases flow through a catalytic converter where the temperature increases from T_6 to by T_7 due to the conversion of unburned particles. The gas leaving the catalytic converter enters a turbine to generate the power needed to drive the compressor. Finally, the exhaust gases leave the turbine at atmospheric pressure and temperature T_9 after having exchanged heat with compressed air in the regenerator.

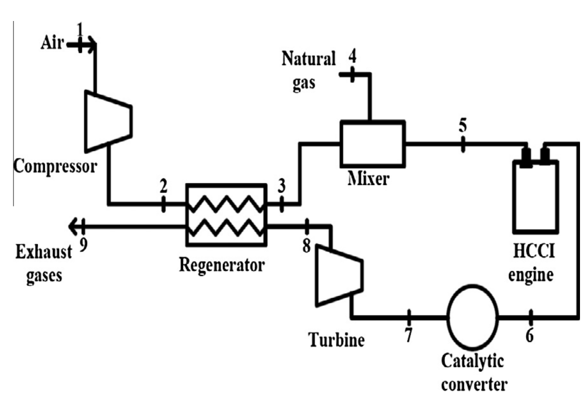

Fig. 1. Scheme of the system studied.

3.2. Energy analysis

Mass and energy balances for any control volume at steady state with negligible kinetic and potential energy changes can be expressed respectively by the following expressions:

$$\begin{cases} \sum \dot{m}_i - \sum \dot{m}_o = 0 \\ Q - W = \sum \dot{m}_o h_o - \sum \dot{m}_i h_i \end{cases} \tag{5}$$

To carry out an energy analysis, the above balance equations should be applied to each component of the system.

The compressor is required to provide a compressed air supply for the engine in order to improve the power and efficiency. The compressor inlet properties (state 1) are calculated knowing T_1 and p_1. For a given pressure ratio, r_p, the compressor outlet properties (state 2) are calculated in two steps:

- First, the temperature at the end of the isentropic compression is determined by the numerical solution of the following equation:

$$s_{2s} = s_1 \tag{6}$$

- Then, the properties at state 2 are calculated using the compression efficiency definition:

$$\eta_{comp} = (h_{2i} - h_1)/(h_2 - h_1) \tag{7}$$

Here again, temperature T_2 is obtained by a numerical inversion method.

An energy balance on the compressor yields

$$w_c = h_2 - h_1 \tag{8}$$

The regenerative heat exchanger (regenerator) is used to heat the compressed air using the exhaust gases. The effectiveness of this heat exchanger is given by:

$$\varepsilon = [(\dot{m} \cdot c_p)_2 (T_3 - T_2)]/[(\dot{m} \cdot c_p)_{\min} (T_8 - T_2)] \tag{9}$$

Temperature at the exit of the regenerative heat exchanger, T_3, is calculated assuming $(\dot{m} \cdot c_p)_2 = (\dot{m} \cdot c_p)_{\min}$ by the following relation:

$$T_3 = T_8 \varepsilon + T_2 (1 - \varepsilon) \tag{10}$$

The application of energy balance on the regenerator yields

$$\mathrm{H}_3 - \mathrm{H}_2 = \mathrm{H}_8 - \mathrm{H}_9 \rightarrow \mathrm{H}_9 = \mathrm{H}_8 - \mathrm{H}_3 + \mathrm{H}_2 \tag{11}$$

Temperature at the exit of the mixer is calculated using energy balance equation:

$$\mathrm{H}_5 = \mathrm{H}_3 + \mathrm{H}_4 \tag{12}$$

The gaseous mixture exiting the mixer enters the HCCI engine whose thermodynamic cycle is modelled by a turbocharged Otto cycle as shown in Fig. 2.

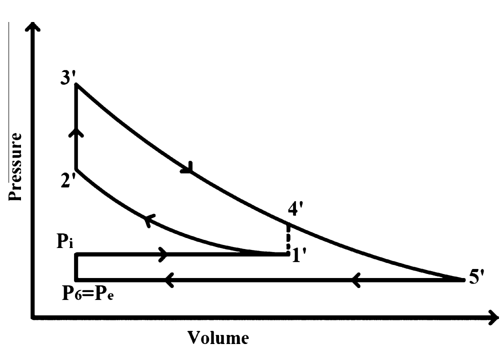

Fig. 2. Otto turbocharged cycle.

Temperature at the end of the intake process $(i - 1')$ is calculated using the following expression [12] :

$$T_{1'} = \frac{T_i(1-f)}{1 - 1/[(n \cdot r_c) p_e/p_i + (n-1)]} \tag{13}$$

where, $p_i/p_e = 1.4$ and f is the residual gases fraction fixed to 0.03 according to the reference cited. n is the average specific heat capacity ratio fixed to 1.35 for lean air–fuel mixtures [12].

The pressure remains unchanged:

$$p_{1'} = p_i \tag{14}$$

During the compression process $(1' - 2')$, the gaseous mixture is heated up to ignition and combustion. For a fixed pressure ratio ($r_c = 16$), properties at state $2'$ can be calculated in a similar manner to state 2 using compression isentropic efficiency.

Properties at the end of the heat supply process $(2' - 3')$ are determined using an inversion numerical method of the following equation:

$$\dot{Q}_{in} = \dot{Q}_{fuel} - \dot{Q}_l \tag{15}$$

where $\dot{Q}_{fuel}$ is the heat supplied to the cycle given by:

$$\dot{Q}_{fuel} = \eta_{comb} \dot{m}_{fuel} Q_{LHV} \tag{16}$$

The losses inside the combustor are taken into account by introducing combustion efficiency [28]:

$$\eta_{comb} = 100 - V_{\%c} - \left(1.26 + 0.25 C_{e2} + 0.4 C_{e2}^2\right) + (\phi - 0.2486) 8.1 \tag{17}$$

where $C_{e2} = Ln(V_{\%c})/Ln(2)$

The heat losses from the in-cylinder gas to the surrounding walls, $\dot{Q}_l$, are calculated using:

$$\dot{Q}_l = h_c \cdot 10^{-3} (A_{ch} + A_{cyl})(T_{avr} - T_w)/(2 \cdot \dot{m}_a) \tag{18}$$

where, A_{ch} is the surface of cylinder head, A_{cyl} is the surface of the cylinder and h_c is the heat transfer coefficient calculated using the following expression [29]:

$$h_c = (3.26 L^{-0.2} p^{0.8} T_{avr}^{-0.73} \omega^{0.8}) \tag{19}$$

where L is the engine stroke. The gas average temperature, T_{avr}, is considered here in absence of information about the instantaneous temperature, and ω is the mean gas velocity within the cylinder:

$$\omega = 2.28 \overline{S}_p + (3.24 e^{-3}/6)(V_d T_{ref} (p - p_{mot})/(p_{ref} V_{ref})) \tag{20}$$

where p_{mot} is the pressure at motored conditions [30]:

$$p_6 = p_r (V_r/V)^n \tag{21}$$

p_r and V_r are the pressure and the volume at a reference state.

The parameters of the working fluid at the end of the expansion process $(3' - 4')$ can be calculated also in similar manner to the compression process $(1' - 2')$.

For a turbocharged engine, the exhaust process $(4' - 1')$ is substituted by an expansion process $(4' - 5')$. The final state parameters (the end of the blow down phase) are calculated using:

$$p_{5'} = p_e \tag{22}$$

$$T_{5'} = T_{4'} (p_{4'}/p_e)^{(1-n)/n} \tag{23}$$

$$v_{5'} = \frac{\overline{R}}{M_{mix}} \frac{T_{5'}}{p_{5'}} \tag{24}$$

Finally, temperature and pressure at the end of the exhaust process $(5' - 6)$ are:

$$T_e = T_{5'} \tag{25}$$

$$p_6 = p_{5'} = p_e \tag{26}$$

The heat released by friction is evaluated using the relation of Wu and Ross [31]:

$$\dot{Q}_f = \dot{m}_t \left(183 + 2.3\left(\left(\frac{N}{60}\right) - N_0\right) V_D\right) \tag{27}$$

with,

$$N_0 = 30\sqrt{3/(1000V_d)} \tag{28}$$

The heat rejected in exhaust gases is calculated using:

$$\dot{Q}_{out} = \dot{m}_t[(h_4 - r \cdot T_4) - (h_5 - r \cdot T_5)] \tag{29}$$

The net power produced by the cycle can be calculated using the following equation:

$$\dot{W}_{net} = \dot{Q}_{in} - \dot{Q}_{out} - \dot{Q}_f \tag{30}$$

The thermal efficiency of the engine, η_{th}, is defined as the ratio of the power produced by the cycle to total energy supplied to the cycle:

$$\eta_{th} = \dot{W}_{net} / \dot{Q}_{in} \tag{31}$$

3.3. Exergy analysis

Traditionally, thermodynamic cycles are analysed using the energy analysis method which is based on the first law of thermodynamics, i.e. the energy conservation concept. Unfortunately, this method cannot locate the degradation of the quality of energy. Instead, exergy analysis which is based on both the first and second laws of thermodynamics can overcome easily the limitations of the energy analysis. Exergy analysis is considered by several researchers as powerful tool for thermodynamic cycles because it helps to determine the true magnitudes of losses and their causes and locations, showing thus where efforts should concentrated to improve the overall system and its components. Furthermore, the total exergy losses can be considered as an optimisation criteria which, by minimisation, provides optimum processes configuration. The concept and the methodology of exergy analysis are well-documented in the literature [32–34].

In absence of nuclear, magnetic, electric and superficiel effects, the exergy of a system is composed of four components: physical, chemical, potential and kinetic.

$$ex = ex^k + ex^p + ex^{ph} + ex^{ch} \tag{32}$$

For engines applications, kinetic and potential contributions are assumed to be negligible compared to physical and chemical exergies. Physical exergy results from temperature and pressure differences from the dead state:

$$ex^{ph} = (h - h_0) - T_0(s - s_0) \tag{33}$$

On the other hand, chemical exergy takes into account deviations in chemical composition from reference substances present in the environment:

$$ex^{ch} = \sum x_i\left(\mu_i^* - \mu_{i,0}\right) = -\Delta g_i^0 + \sum \overline{R} T_0 x_i \ln\left(\frac{p}{p_{ref}}\right) \tag{34}$$

where, μ_i and g_i are the chemical potential and the Gibbs function of species i evaluated at a temperature T and pressure p.

Exergy is always evaluated with respect to a reference environment (dead state).

The exergy destroyed in a system originate from the internal irreversibilities. It can be calculated using the global exergy balance in steady state [35]:

$$\begin{aligned}\Delta\dot{E}x &= \sum \dot{E}x_i - \sum \dot{E}x_o \\ &= \sum\left(1 - \frac{T_0}{T_j}\right)\dot{Q}_k - \dot{W}_{CV} + \sum \dot{m}_i ex_i - \sum \dot{m}_o ex_o\end{aligned} \tag{35}$$

where $\sum \dot{E}x_i$ and $\sum \dot{E}x_o$ are the destroyed, input and output exergy rates, respectively, $\dot{m}$ is the mass flow rate of a stream of matter, and $\dot{Q}_k$ and $\dot{W}_{CV}$ the energy rates transfer by heat and work. The subscripts i and o denote inlet and outlet and the subscript k the boundary of the component of interest.

Instead, the exergy destruction rate can be determined using the Gouy–Stodola formula:

$$\Delta\dot{E}x = T_0\dot{S}_{gen} \tag{36}$$

where $\dot{S}_{gen}$ is the entropy generation rate.

From a second law point of view, it is important to quantify the exergy losses in each component in order to assess the overall performance of the system. To assess the contribution of each component of the system in the total exergy losses, exergy balance equation is applied to each component. The expressions allowing the calculation of individual exergy losses of each component of the system and their exergy efficiencies are summarised in Table 1.

Exergy losses are generated in all the components of the system, namely the compressor, the regenerator, the mixer, the HCCI engine, the turbine and the catalytic converter. Thus, the total exergy losses $\Delta\dot{E}x_{tot}$ may be written as the sum of individual losses occurring in these components, i.e.,

$$\begin{aligned}\Delta\dot{E}x_{tot} &= \Delta\dot{E}x_{comp} + \Delta\dot{E}x_{reg} + \Delta\dot{E}x_{mix} + \Delta\dot{E}x_{HCCI} + \Delta\dot{E}x_{tur} \\ &\quad + \Delta\dot{E}x_{cat}\end{aligned} \tag{37}$$

The exergy loss in the HCCI engine is the sum of exergy losses occurring in the compression process, $\Delta\dot{E}x_c$, the exergy loss of the combustion process, $\Delta\dot{E}x_{cc}$, the exergy loss during the expansion, $\Delta\dot{E}x_{\exp}$, the exergy loss during the exhaust gas phase, $\Delta\dot{E}x_e$, and the exergy of the gas, $\Delta\dot{E}x_{gas}$.

Table 1
Individual exergy losses and efficiencies of the system components.

Component	Exergy loss	Exergy efficiency
Compressor	$\dot{W}_{comp} + \dot{m}_a\left(ex_1^{ph} - ex_2^{ph}\right)$	$\dot{m}_a\left(ex_2^{ph} - ex_1^{ph}\right)/\left(-\dot{W}_{comp}\right)$
Regenerator	$\dot{m}_a(ex_2^{ph} - ex_3^{ph}) + \dot{m}_t\left(ex_8^{ph} - ex_9^{ph}\right)$	$\left[\dot{m}_a\left(ex_3^{ph} - ex_2^{ph}\right)\right]/\left[\dot{m}_t\left(ex_8^{ph} - ex_9^{ph}\right)\right]$
Mixer	$\dot{m}_a ex_3^{ph} + \dot{m}_f ex_4^{ph} - \dot{m}_t ex_5^{ph}$	$\left(\dot{m}_a ex_3^{ph}\right)/\left(\dot{m}_f ex_4^{ph} - \dot{m}_t ex_5^{ph}\right)$
HCCI engine	$\dot{m}_t\left(\Delta ex_c + \Delta ex_{cc} + \Delta ex_{\exp} + \Delta ex_e + \Delta e_{gas}^{ch}\right)$	$\dot{W}_{net}/\dot{E}x_{fuel}$
Turbine	$\dot{m}_t\left(ex_7^{ph} - ex_8^{ph}\right) - \dot{W}_{tur}$	$\dot{W}_{tur}/\left[\dot{m}_t\left(ex_7^{ph} - ex_8^{ph}\right)\right]$
Catalytic converter	$\dot{m}_t\left(ex_6^{ph} - ex_7^{ph} + ex_{cat}^{ch}\right)$	$\left(\dot{m}_t ex_7^{ph}\right)/\left[\dot{m}_t\left(ex_6^{ph} + ex_{cat}^{ch}\right)\right]$

The exergy efficiency is a criterion for thermodynamic perfection of a process and can be defined as the ratio of the product of a process to the required input of fuel, both of which are expressed in exergy units:

$$\eta_{ex} = \frac{\dot{E}x_{product}}{\dot{E}x_{fuel}} \tag{38}$$

The term "product" represents the desired output of a process and "fuel" refers to the resource that is used to generate this output, which only in some cases is an actual fuel. The exergy efficiency shows the percentage of the fuel exergy that is transferred to product exergy.

4. Results and discussions

This section includes a comprehensive performance analysis of a homogeneous charge compression ignition engine based system using natural gas as fuel. The system has been simulated under steady-state conditions. The second law of thermodynamics has been mainly used in order to evaluate the exergy losses and efficiencies. For both energy and exergy analyses, the engine has been considered to be a control volume and a steady-state open system. Furthermore, air and combustion products are considered as ideal gases.

A Fortran program for calculating the system performance has been developed using analytical equations and empirical correlations presented in the above section. As mentioned, the model considers real compression and expansion processes and heat transfer losses. After the determination of the working fluid properties at each point of the system represented in Fig. 1, the calculation of the engine performance can be carried out. Using appropriate operating data typical for HCCI engines and chosen according to the literature, exergy losses in each device of the system and the overall exergy efficiency of the system at a reference temperature of 25 °C have been determined. Results have been obtained based on engine compression ratio equal to 16. Table 2 shows the operating conditions of the system shown in Fig. 1.

Table 2
Operating conditions.

Ambient temperature, K	290–310
Ambient pressure, kPa	101.325
Compressor efficiency	0.7–0.9
Turbine efficiency	0.7–0.9
Engine compression ratio	16
Residual gases fraction	0.03
Equivalence ratio	0.3–0.9
Compressor compression ratio	2.5–3.5
Wall temperature, K	400

Fig. 3 represents the variation of thermal and exergetic efficiency values of the HCCI engine with respect to compressor compression ratio for three ambient temperatures: 290, 300 and 310 K. Both thermal and exergetic efficiencies are found increasing with increasing compression ratio. This increase is due to the improvement the mixing of fuel and air, which raises the temperature of the mixture and enhances the combustion reaction. Qualitatively, exergetic efficiencies behave similarly to thermal efficiencies, but exhibit much lower magnitudes due to higher fuel exergy compared to fuel energy. It is evident that exergy efficiency provides an indication of the potential for improvement that is more fundamental than that shown by thermal efficiency. On the other hand, the increase of the ambient temperature involves a decrease of the system efficiencies. This decrease is due to a reduction in the volumetric efficiency. The increase of ambient temperature requires more fuel consumption in the combustion chamber. Hence, from both energy and exergy points of view, it is more suitable to operate the system at lower ambient temperature. The variation of inlet air temperature can be achieved by controlling the amount of exhaust gases that enter the regenerator using controllable valve.

In Fig. 4, the effects of changing fuel–air equivalence ratio are examined for three different engine speeds: 1200, 1800 and 2400 rpm. The equivalence ratio is the primary parameter that determines the supplied energy. Higher equivalence ratios allow more energy release resulting in an increase of in-cylinder temperature and pressure. Higher in-cylinder pressures and temperatures lead to increased power produced by the engine, thereby improve both thermal and exergetic efficiencies. A higher engine speed increases the charge-flow intensity and improves the mixing of fuel and air. In addition to its effect on in-cylinder temperature and pressure, the engine speed affects the wall temperature of the combustion chamber. The increase of the engine speed reduces the duration of cycle evolution and causes a reduction of the heat loss to the cylinder wall. Moreover, heat losses in exhaust gases decrease with increasing engine speeds. Finally, friction effects at low speeds are lower than that at higher speeds. In conclusion, the thermal and exergetic efficiencies increase as engine load increases due largely to the decreasing of heat losses. The effect of engine speed is lower.

A mapping of exergy losses in the whole system is performed for various operating conditions. Individual exergy losses are expressed as percentages of the total exergy losses. The results in Table 3–6 show how the more important parameters, such as the compressor compression ratio, the equivalence ratio, the ambient temperature and the engine speed affect the exergy losses and the exergetic efficiencies of the components of the system.

First, exergy losses of the components of the system for various values of the compressor pressure ratio at an ambient temperature of 300 K, an equivalence ratio of 0.5 and an engine speed of 1800 rev/min have been calculated (Table 3). The results show that

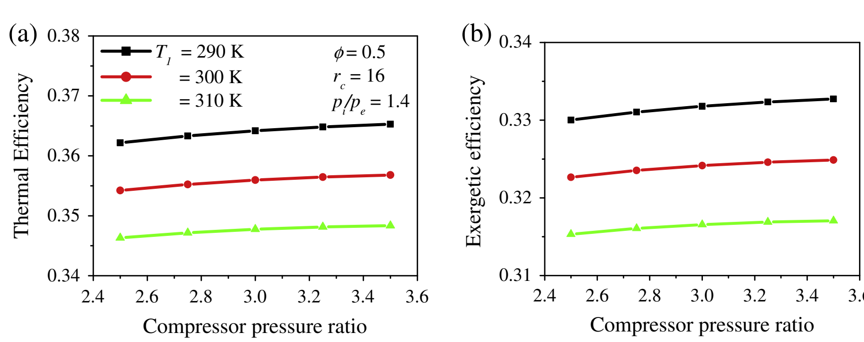

Fig. 3. Combined effects of compressor pressure ratio and ambient temperature on the system performance: *a*. Thermal efficiency; *b*. Exergetic efficiency.

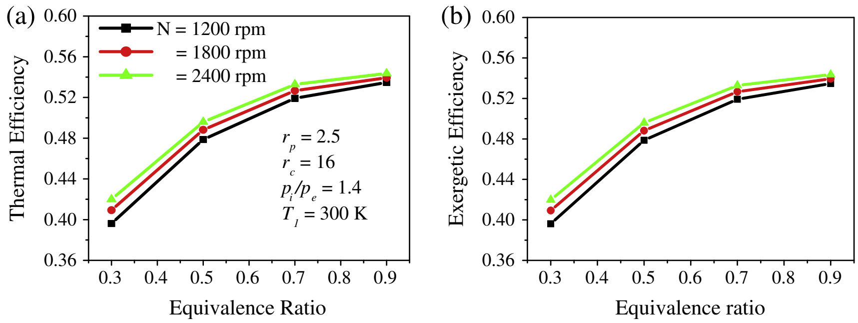

Fig. 4. Combined effects of equivalence ratio and engine speed on the system performance: (a). Thermal efficiency; (b). Exergetic efficiency.

Table 3
Effect of the compressor pressure ratio on exergy losses and efficiencies of the system components.

r_p		Compressor	Regenerator	Mixer	HCCI	Catalytic	Turbine
2.5	Exergy loss, %	2.35	0.88	0.18	86.10	8.92	1.56
	Exergy efficiency, %	82.83	73.28	96.22	29.97	69.59	85.11
3	Exergy loss, %	2.75	0.49	0.19	86.10	8.49	1.98
	Exergy efficiency, %	83.33	80.28	96.29	30.02	72.65	85.21
3.5	Exergy loss, %	3.07	0.25	0.20	86.04	8.12	2.31
	Exergy efficiency, %	83.72	85.96	96.34	30.00	74.94	85.30

Table 4
Effect of the engine speed on exergy losses and efficiencies of the system components.

N		Compressor	Regenerator	Mixer	HCCI	Catalytic	Turbine
1200	Exergy loss, %	1.05	1.30	0.37	89.43	7.24	0.60
	Exergy efficiency, %	82.83	66.18	32.77	47.86	48.41	90.02
1800	Exergy loss, %	1.04	1.34	0.37	89.45	7.21	0.59
	Exergy efficiency, %	82.83	66.33	33.34	48.82	49.15	90.13
2400	Exergy loss, %	1.03	1.36	0.37	89.47	7.18	0.58
	Exergy efficiency, %	82.83	66.21	33.38	49.59	49.72	90.30

Table 5
Effect of the equivalence ratio on exergy losses and efficiencies of the system components.

ϕ		Compressor	Regenerator	Mixer	HCCI Engine	Catalytic converter	Turbine
0.5	Exergy loss, %	1.04	1.34	0.37	89.45	7.21	0.59
	Exergy efficiency, %	82.83	66.32	33.34	30.02	49.15	90.21
0.7	Exergy loss, %	0.82	1.86	0.52	89.51	6.91	0.37
	Exergy efficiency, %	82.83	64.41	43.53	30.00	59.45	93.6
0.9	Exergy loss, %	0.61	2.69	0.74	84.74	11.31	0.18
	Exergy efficiency, %	82.83	64.37	61.96	30.00	39.16	97.13

over the range of pressure ratios explored, the greatest exergy losses occur in the HCCI engine. Irreversible processes occurring in the HCCI engine causes between 86.04% and 86.10% of total exergy losses in the system. Exergy losses in the HCCI engine originate mainly from the irreversible combustion process. During this process, an increased internal heat exchange occurs to raise the temperature of increased amounts of non-reactive species. Losses in the others components of the system are minimums, indicating that there is no potential for improvement under the operating parameters considered. For example, for a pressure ratio of 2.5, the amount of exergy losses in the catalytic converter, the compressor, the turbine, the regenerator and the mixer represent 8.9%, 2.35%, 1.56%, 0.88% and 0.17% respectively.

Finally, it is interesting to mention that within the range of operating parameters considered, exergy losses and exergy efficiencies of the compressor, the mixer and the turbine exhibit a special behavior. Both increases with increasing the compressor pressure ratio.

Similarly, individual exergy losses, expressed as a percentage of the total exergy loss, have been evaluated as a function of the engine speed. It can be observed from Table 4 that with the increase of the engine speed, percentages of exergy losses of the regenerator and the HCCI engine increase. However, percentages of exergy losses of the catalytic converter and the turbine decrease with the increase of the engine speed, while percentages of exergy losses occurring in the compressor and the mixer are slightly

Table 6
Effect of ambient temperature on exergy losses and efficiencies of the system components.

T_1		Compressor	Regenerator	Mixer	HCCI Engine	Catalytic converter	Turbine
290	Exergy loss, %	1.47	0.63	0.20	89.07	7.64	0.98
	Exergy efficiency, %	82.29	70.31	18.15	41.77	25.78	84.40
300	Exergy loss, %	1.43	0.55	0.22	89.15	7.67	0.97
	Exergy efficiency, %	82.83	73.22	20.60	40.93	27.19	84.68
3100	Exergy loss, %	1.43	0.49	0.23	89.21	7.69	0.96
	Exergy efficiency, %	83.34	75.82	22.99	40.10	28.54	84.94

affected by the variation of the engine speed. Again, the exergy loss in the HCCI engine is considerably larger than exergy losses in the others components. For example, for an engine speed of 1800 rpm, it counts alone for 89.45% of total exergy losses in the system, while the exergy loss rate of the compressor, the regenerator, the mixer, the catalytic converter and the turbine are only 1.04%, 1.34%, 0.37%, 7.21% and 0.59%, respectively. The exergy losses in the system are mainly due to the irreversible nature of the combustion process, heat transfer through a finite temperature difference, friction and mixing process.

The equivalence ratio defines the level of in-cylinder gas temperature after combustion, thus it affects the amount of combustion exergy losses generated. Richer air–fuel mixtures increase the chemical exergy supplied to the engine. The exergy losses and exergetic efficiencies of all components are also calculated four several values of equivalence ratios and their comparison is depicted in Table 5. Exergy losses and exergy efficiencies are determined for equivalence ratios ranging from 0.5 to 0.9. As seen in the table, the most significant of all the exergy losses remains the HCCI engine. However, in contrast to the previous results, it is shown that exergy losses in the HCCI engine increase than decrease for higher equivalence ratios. A different trend is also observed for exergy losses in the catalytic converter. They decrease than they increase for higher equivalence ratios.

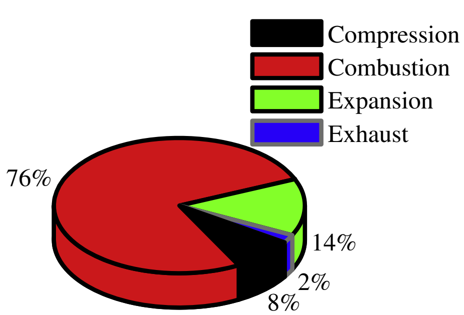

Fig. 5. HCCI engine exergy losses mapping during a cycle.

The sensitivity of individual exergy losses and exergy efficiencies for the main components of the system to the variation of the ambient temperature is shown in Table 6. The HCCI engine produces the largest amount of exergy losses. They represent more than 89% of the total exergy losses. These losses are mainly due to the combustion process. The other components, namely the compressor, the regenerator, the mixer, the catalytic converter and the turbine contribute with values less than 1.47, 0.63, 0.23, 7.69 and 0.98 of total exergy destruction, respectively.

Since exergy losses of the HCCI engine are dominant over all the other exergy losses in the system, they have been examined in more detail. Fig. 5 illustrates an exergy losses mapping of the HCCI engine at an ambient temperature of 300 K, a compressor pressure ratio of 2.5, an equivalence ratio of 0.5 and an engine speed of 1800 rev/min. It can be seen that the combustion process creates the highest contribution to the total exergy losses in the HCCI engine, which represent in the present case 76%. This can be explained by the fact that chemical reaction occurring during the combustion process increases the entropy of the resulted gases. The exergy loss during the combustion process is the penalty of converting the fuel exergy to thermal energy for producing work. Compared to the combustion process, the rate of exergy losses are smaller during the expansion stroke (14%), the compression stroke (8%) and the exhaust process (2%). As a result, large potential can be achieved to improve the system efficiency by reducing exergy losses during the combustion process.

Generally, the isentropic efficiency of compressors and turbines ranges from 70% to 90%. Fig. 6 shows the effect of compressor and turbine isentropic efficiencies on thermal and exergetic efficiencies of the HCCI engine for different values of the effectiveness of the regenerator. For simplicity, the turbine and compressor isentropic efficiencies are considered equal. As expected, the increase of compressor and turbine efficiencies and regenerator effectiveness increases slightly both the thermal and exergetic efficiencies of the HCCI engine. This tendency is due to decreased irrevrsibilities

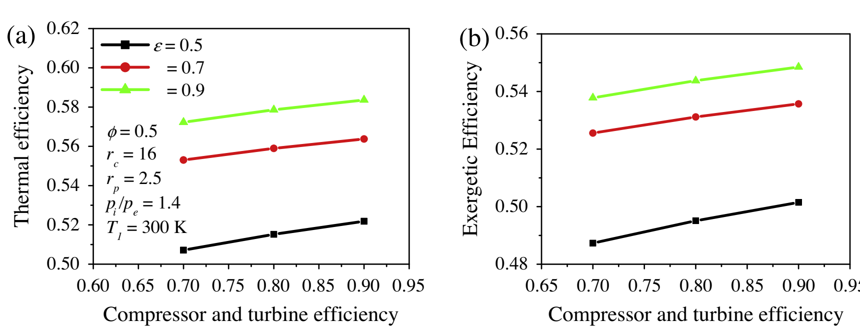

Fig. 6. Combined effects of compressor and turbine isentropic efficiencies and regenerator effectiveness on the HCCI performance: (a). Thermal efficiency; (b). Exergetic efficiency.

for higher turbine and compressor efficiencies. Similar trend is observed for higher values of effectiveness. Higher values of effectiveness also decrease exergy losses in the regenerator.

5. Conclusions

Energy and exergy analysis of a thermal system based on a turbocharged HCCI engine fuelled with natural gas has been carried out. The working fluid is considered as a mixture of gases with variable specific heats.

The system performance have been determined and analysed by numerical examples as a function of the compressor pressure ratio, compressor isentropic efficiency, ambient temperature, equivalence ratio, engine compression ratio and the engine speed. The results showed that the operating parameters mentioned above have a significant impact on the system performance:

– Both thermal and exergetic efficiencies are found increasing with increasing compressor compression ratio.
– The increase of ambient temperature involves a decrease of the engine efficiencies.
– Higher equivalence ratios allow more energy release resulting in an increase of both thermal and exergetic efficiencies.
– The increase of the engine speed improves slightly both thermal and exergetic efficiencies.

The present study confirmed the advantage of exergy analysis as compared to energy analysis. The amount of information gained through the mapping of exergy losses in the system leads to better understanding of exergy flow in the system in order to improve the overall efficiency of the system. The effects of compressor pressure ratio, engine speed, equivalence ratio and ambient temperature show different tendencies with diverse magnitude. The comparison between exergy losses of the individual component showed that the HCCI engine represents a potential component that can be improved in order to improve the overall system efficiency. Most of exergy losses during the cycle accomplishment are due to the irreversible nature of the combustion process.

It is also shown that within the range of operating parameters considered, exergy losses and exergy efficiencies for some cases exhibit a special behavior. Both increases with increasing the compressor pressure ratio, the engine speed, the equivalence ratio or the ambient temperature.

References

[1] CNSS. A review of present technological solutions for clean shipping; 2011. <www.cleantech.cnss.no>.
[2] Zhao F, Asumus T, Assanis D, Dec J, Eng J, Najt P. Homogeneous charge compression ignition (HCCI) engines: key research and development issues; PT-94. Warrendale (PA): Society of Automotive Engineers; 2003.
[3] Alkidas AC. Combustion advancements in gasoline engines. Energy Convers Manage 2007;48:2751–61.
[4] Cho HM, He BQ. Spark ignition natural gas engines—a review. Energy Convers Manage 2007;48:608–18.
[5] U.S. Department of Energy. Alternative Fuels Data Center, Fuel properties; 2012. <http://www.afdc.energy.gov/fuels/properties.html>
[6] Karila K, Kakkanen T, Larmi M, Niemi S, Sandstro CE, Tamminen J, et al. Reduction of particulate emissions in compression ignition engines. Espoo (Finland): Publication of the Internal Combustion Engine Laboratory, Helsinki Unviersity of Technology; 2004.
[7] Zheng J, Caton JA. Use of single-zone thermodynamic model with detailed chemistry to study a natural gas fueled homogeneous charge compression ignition engine. Energy Convers Manage 2012;53:298–304.
[8] Thring RH. Homogeneous charge compression ignition (HCCI) engines. SAE paper no. 892068; 1989.
[9] Kong SC, Reitz RD. Numerical study of premixed HCCI engine combustion and its sensitivity to computational mesh and model uncertainties. Combust Theor Model 2003;7:417–33.
[10] Osborne RJ, Li G, Sapsford SM, Stokes J, Lake TH, Heikal MR. Evaluation of HCCI for future gasoline powertrains. SAE technical paper 2003-01-0750; 2003.
[11] Aceves SM, Flowers DL, Martinez-Frias J, Martinez-Frias J Dec JE, Sjöberg M, et al. Spatial analysis of emissions sources for HCCI combustion at low loads using a multi-zone model. SAE paper 2004-01-1910; 2004.
[12] Zheng ZQ, Yao MF, Chen Z, Zhang B. Experimental study on HCCI combustion of dimethyl ether (DME)/methanol dual fuel. SAE paper 2004-01-2993; 2004.
[13] Komninos NP, Hountalas DT, Kouremenos DA. Development of a new multi-zone model for the description of physical processes in HCCI engines. SAE Paper 2004-01-0562; 2004.
[14] Su WH, Huang HZ. Development and calibration of a reduced chemical kinetic model of n-heptane for HCCI engine combustion. Fuel 2005;84:1029–40.
[15] Hu T, Liu S, Zhou L, Li W. Effects of compression ratio on performance, combustion, and emission characteristics of an HCCI engine. Proc Inst Mech Eng, Part D: J Automobile Eng 2006;220:637–45.
[16] Wang Z, Wang JX, Shuai SJ, Tian GH, An X, Ma QJ. Study of the effect of spark ignition on gasoline HCCI combustion. Proc Inst Mech Eng, Part D: J Automobile Eng 2006;220:817–25.
[17] Szybist JP, McFarlane J, Bunting BG. Comparison of simulated and experimental combustion of biodiesel blends in a single cylinder diesel HCCI engine. SAE paper 2007-01-4010; 2007.
[18] Sato S, Yamashita D, Iida N. Influence of the fuel compositions on the homogeneous charge compression ignition combustion. Int J Eng Res 2008;9:123–48.
[19] Liu H, Yao M, Zhang B, Zheng Z. Influence of fuel and operating conditions on combustion characteristics of a homogeneous charge compression ignition engine. Energy Fuel 2009;23:1422–30.
[20] Bedoya ID, Saxena S, Cadavid FJ, Dibble RW, Wissink M. Experimental study of biogas combustion characteristics and emissions in a HCCI engine for power generation. Energy Convers Manage 2011;53:154–62.
[21] Visakhamoorthy S, Tzanetakis T, Haggith D, Sobiesiak A, Wen JZ. Numerical study of a homogeneous charge compression ignition (HCCI) engine fueled with biogas. Appl Energy 2012;92:437–46.
[22] Bahlouli K, Atikol U, Saray RK, Mohammadi V. A reduced mechanism for predicting the ignition timing of a fuel blend of natural-gas and n-heptane in HCCI engine. Energy Convers Manage 2014;79:85–96.
[23] Soylu S. Examination of combustion characteristics and phasing strategies of a natural gas HCCI engine. Energy Convers Manage 2005;46:101–19.
[24] Khaliq A, Trivedi SK, Dincer I. Investigation of a wet ethanol operated HCCI engine based on first and second law analyses. Appl Therm Eng 2012;31:1621–9.
[25] Khaliq A, Trivedi SK. Second law assessment of a wet ethanol fuelled HCCI engine combined with organic Rankine cycle. ASME J Energy Resour Technol 2012;143:1–12.
[26] Saxena S, Shah N, Bedoya I, Phadke A. Understanding optimal engine operating strategies for gasoline-fueled HCCI engines using crank-angle resolved exergy analysis. Appl Energy 2014;114:155–63.
[27] Glassman I, Yetter RA. Combustion. 4th ed. USA: Elsevier; 2008.
[28] Mo Y. HCCI heat release rate and combustion efficiency: a coupled kiva multi-zone modeling study. PhD Thesis, University Michigan, USA; 2002.
[29] Soyhan HS, Yasar H, Head B, Kalghatgi GT, Sorusbay C. Evaluation of heat transfer correlations for HCCI engine modeling. Appl Therm Eng 2009;29:541–9.
[30] Heywood JB. Internal combustion engine fundamentals. New York: McGraw-Hill; 1988.
[31] Olof E. Thermodynamic simulation of HCCI engine systems. PhD Thesis, Lund University, Sweden; 2002.
[32] Kotas TJ. The exergy method of thermal plant analysis. 1st ed. London: Butterworth; 1985.
[33] Brodyansky VM, Sorin MV, Le Goff P. The efficiency of industrial processes: exergy analysis and optimization. New York: Elsevier; 1994.
[34] Moran MJ, Shapiro HN. Fundamentals of engineering thermodynamics. 4th ed. New York: Wiley; 2000.
[35] Bejan A, Tsatsaronis G, Moran M. Thermal design & optimization. New York, USA: John Wiley & Sons; 1996.